11TH INTERNATIONAL SYMPOSIUM FIELD MONITORING IN GEOMECHANICS

Interpretation of Distributed Rayleigh Sensing Data for Slope Stability and Ground Condition Monitoring

Paul CLARKSON[1], Roger CRICKMORE[1], Steve COLE[1], Alastair GODFREY[1], Chris MINTO[1], Arnaud WATLET[2], James WHITELEY[2], Ben DASHWOOD[2] and Jonathan CHAMBERS[2]

[1]OptaSense, Farnborough, United Kingdom
[2]British Geological Survey, Nottingham, United Kingdom
Corresponding author: Paul Clarkson (paul.clarkson@optasense.com)

Abstract

A novel ground condition and slope stability monitoring system based on Distributed Rayleigh Sensing (DRS) has been developed. This system uses the backscattered light from buried fibre optic cables to determine the strain and temperature at any point along the fibre up to distances of over 50 km. In addition to long-term strain and temperature measurements, the system can also sense acoustic vibrations and can be used to make active and passive seismic surveys to give a comprehensive 3d picture of the subsurface state. Changes in ground condition and stress state detected on the fibre may be useful predictors for slope failure and ground movement and can be detected within seconds, allowing alerts to be generated and action to be taken.

The system is installed in the near surface of a slope at the British Geological Survey's national landslide observatory and has been shown to respond to a range of environmental and geotechnical changes. This paper examines the parameters that can be derived from the output of the fibre and interprets the output over a range of timescales considering the relationship with the properties of the ground. These properties include moisture content, ground movement, thermal diffusivity and seismic depth velocity profiles obtained from active and passive surveys using the fibre.

The slope is also monitored with a range of other instrumentation, including moisture content sensors, Electrical Resistivity Tomography (ERT), GPS marker posts, temperature sensors, tiltmeters, LiDAR scans and geophones. This provides an excellent test bed for the technology and the additional information from the sensors can be used to aid the interpretation of the DRS system output.

Keywords: Slope Stability, Distributed Fibre Optic Sensing, Seismic Analysis

1. Introduction

Slope stability monitoring is important for failure detection and prediction and for greater understanding of slope behaviour. Slope stability depends on several slope characteristics and there are a wide range of measurement methods that can increase such understanding. Fibre optic based sensing approaches are widely used for infrastructure monitoring and are increasingly being used for structural integrity and slope stability assessment due to their high sensitivity and spatial coverage and resolution. Such systems usually either operate at acoustic frequencies (as in Distributed Acoustic Sensing (DAS) systems) or at lower frequencies as Distributed Strain Sensing (DSS) systems. DAS systems operate by monitoring phase changes in Rayleigh backscattered light from pulses transmitted down an optical fibre. These phase changes occur due to small strains, and temperature induced variations in the refractive index of the fibre. Most systems based on Rayleigh sensing are AC coupled to strain and are not used to perceive strain changes over longer timescales. As such, they have primarily been used for event detection and until recently had limited applicability for longer term condition monitoring and event prediction. However, recent advances in the technology have enabled absolute strain changes to be measured over much longer timescales using Distributed Rayleigh Sensing (DRS) systems. This leads to a wider range of applications, for example slope stability monitoring.

A DRS system has been monitoring long and short-term activity on a slope prone to landslides that is used as the British Geological Survey's (BGS's) landslide observatory at Hollin Hill since October 2020. The slope has been studied extensively using a range of novel and conventional approaches including geomorphological mapping, LiDAR scanning, seismic refraction tomography (SRT), multichannel analysis of surface waves (MASW), self-potential (SP) and electrical resistivity tomography (ERT) to monitor slope hydrology, ground movement and condition changes (e.g. Uhlemann et al., 2017). Previous papers (e.g. Clarkson et al., 2021b) have presented some of the capabilities of the system and illustrated the wide range of parameters that can be measured or

inferred by the system. This paper seeks to expand on this work and further demonstrate the flexibility and range of the system, by presenting examples of thermal diffusivity measurement, pressure sensitivity and sub-surface conditions from seismic depth profiling.

2. Hollin Hill Landslide Observatory and Measurement Systems

2.1 DRS System

The DRS system consists of an interrogator unit (IU) housing a laser source that generates coherent laser pulses that are sent along an optical fibre. The fibre acts as a distributed interferometer, where the phase of backscattered light from different sites along the fibre varies as the fibre is strained and/or the refractive index and therefore optical path length at those points changes. The refractive index depends on both the strain and temperature of the fibre and therefore a measurement of the phase change of the backscattered light between successive pulses can be used to determine changes in strain and temperature. These quantities can be separated by using two fibres running parallel to one another and having different responses to strain and temperature (Crickmore, Minto and Godfrey, 2020). Measurements were made almost simultaneously at multiple points along the fibre spaced 1 metre apart, although each was made over a 4 metre section of fibre so there is 75 % overlap between adjacent samples.

2.2 Fibre Route

The IU and datalogging and control systems are housed in a barn near the Hollin Hill slope. The fibre on the slope is linked to the IU via a tight buffered cable, approximately 700 m long. An overview of the part of the fibre route covering the slope is shown in Figure 1, below. Channel numbers marked on Figure 1 correspond to approximately the same cable distance in metres. Channels 1 to 1807 consist of tight buffered cable, which is responsive to strain and temperature, and channels 1808 to 1950 consist of loose tube cable, which has a strain response of around 10 % of the tight buffered cable and a similar temperature response. Strain measurements made in the section of fibre marked “Dual fibre” in Figure 1 are compensated for temperature, strain measurements in the rest of the fibre include the effects of temperature. In addition to the fibre optic cable, the slope is instrumented with an ERT system, a weather station, tiltmeters, geophones and point reflectors. Regular LIDAR scans are also taken of the site. An overview of the location of various sensors is also shown in Figure 1.

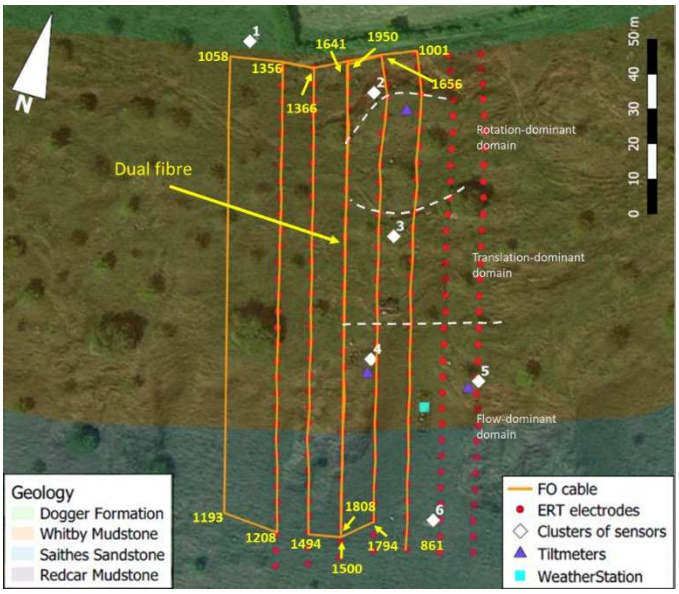

Figure 1: Fibre route and instrumentation at Hollin Hill.

3. Measured parameters

The DRS system is sensitive to static and dynamic strain, vibration, and temperature. The frequency range, spatial resolution and sensitivity to these quantities allow a wide range of ground condition and geological parameters to be studied. A review of some of these properties and how the DRS system can be used to extract them is given in this section.

Strain induced by moisture content changes and ground movement

The direct-buried fibre is very sensitive to changes in ground properties and movement, for example, changes in ground moisture content result in strain changes on the fibre caused by soil shrinkage or pore pressure changes; this behaviour was previously reported in Clarkson et al., 2021b (2021b). Once the moisture content reaches a certain level, the slope becomes unstable and begins to slide. This results in increased strain on the fibre in regions of the slope where the ground becomes separated and decreased strain in regions where material builds up and the fibre is compressed. Examples of strain changes induced by rainfall and ground movement are shown in Figure 2. The image on the left shows the rate of change of strain on the fibre, calculated using samples 4 minutes apart, over a 5-day period including several periods of rainfall. Red on the image indicates increasing strain and blue indicates decreasing strain, a clear decrease in strain is seen when rain occurs.

The image on the right of Figure 2 shows the strain change from 11th January 2021 to 25th January 2021 mapped onto the slope; the strain change caused by rainfall induced ground movement during a large storm is clearly visible. Longer term measurements of ground movement made using GPS measurements of marker posts have shown that the strain on the fibre correlates well with ground movement (Clarkson et al., 2021a).

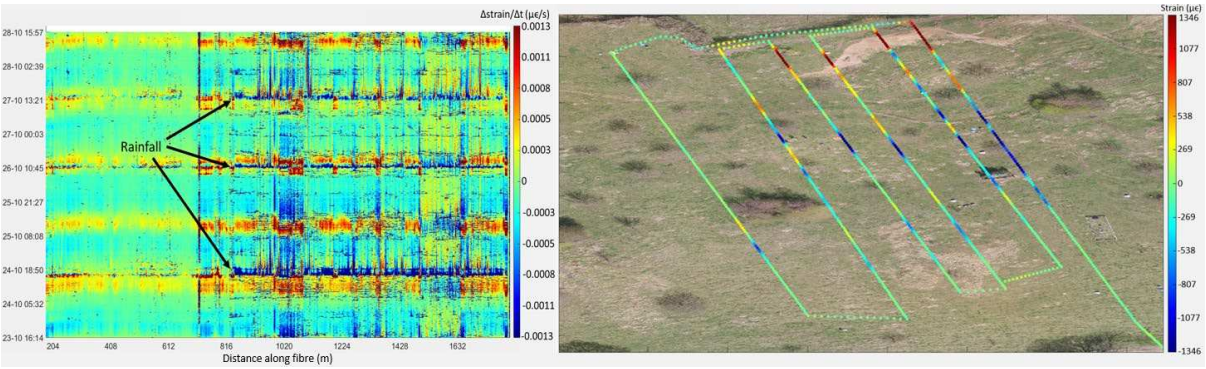

Figure 2: Left – rate of change of strain waterfall image showing rainfall induced strain changes from 23rd October 2020 to 28th October 2020. Right: Cumulative strain change measured between 11th January 2021 and 25th January 2021 mapped onto the slope; most of the strain changes in the right-hand image are a result of ground movement during a landslide caused by heavy rain during a storm.

The strain on the fibre is dependent on coupling of the fibre to the cable, cable geometry and the coefficient of thermal expansion of the cable. The effects of all of these can be measured in the laboratory, but it is more difficult to assess the coupling of the ground to the cable, which also affects the measured strain. As explained in Clarkson et al., 2021a, an average strain over a length between GPS marker posts in the direction of the fibre can be estimated based on the relative movements of the posts to give an indication, but variations in depth and more localised bending, etc, make a precise determination difficult. Further complications arise from the thermal expansion in tight buffered strain sensitive cables being transferred to the fibre. The temperature coefficient of the fibre can be modified to include this effect, but the thermal expansion is reduced when placed in the ground, leading to further uncertainty. Further assessment can be made based on data gathered in the field, for example by comparing measured diurnal temperature variations on loose tube and tight buffered cables, during periods where the strain on the fibre is likely to be relatively constant.

Thermal diffusivity

The thermal diffusivity of the ground can be assessed by observing the thermal response on the fibre compared to the air temperature or fibre above ground. A known temperature change on the surface will result in a delayed thermal response in buried fibre as the heat takes time to propagate through the ground. For periodic temperature changes, such as diurnal changes, the phase and amplitude change of the measured temperature is related to the diffusivity by the following equation (Andújar Márquez, Martínez Bohórquez and Gómez Melgar, 2016),

$$T_{soil}(z,t) = T_m - T_p e^{-z\sqrt{\frac{\omega}{2\alpha}}} cos\left(\omega t - \varphi - z\sqrt{\frac{\omega}{2\alpha}}\right) \quad (1)$$

Where $T_{soil}(z,t)$ is the soil temperature at time t and burial depth z, T_m is the average ambient temperature, T_p is the amplitude of the ambient diurnal temperature variation, ω is the angular frequency (equal to 2π*(1/86400) for daily variations), φ is the phase of the ambient temperature and α is the thermal diffusivity. α can therefore be calculated at a given depth by measuring the phase shift between the ambient temperature and the temperature in the ground over a given period, as shown in equation 2,

$$\alpha = \frac{\omega z^2}{2\vartheta^2} \tag{2}$$

where ϑ is the phase shift between the ambient temperature and the temperature at depth z.

To test the technique the delay in response of a fibre buried in the ground at a site in southern England, relative to air temperature was calculated and the diffusivity was inferred from the phase difference and the burial depth of 50 cm. Figure 3 shows the times of the maxima in the diurnal temperature cycle over a three week period for the fibre and air temperatures. As expected, the air temperature peaked between 14.00 and 15.00 local time, but the fibre temperature did not do so until just after midnight. This difference represents phase shift of about 2.9 radians which implies a thermal diffusivity of around 1.2×10^{-6} $m^2 s^{-1}$. There was a small amount (14 mm) of rainfall over the latter part of the measurement but this did not seem to have a significant effect on the diffusivity.

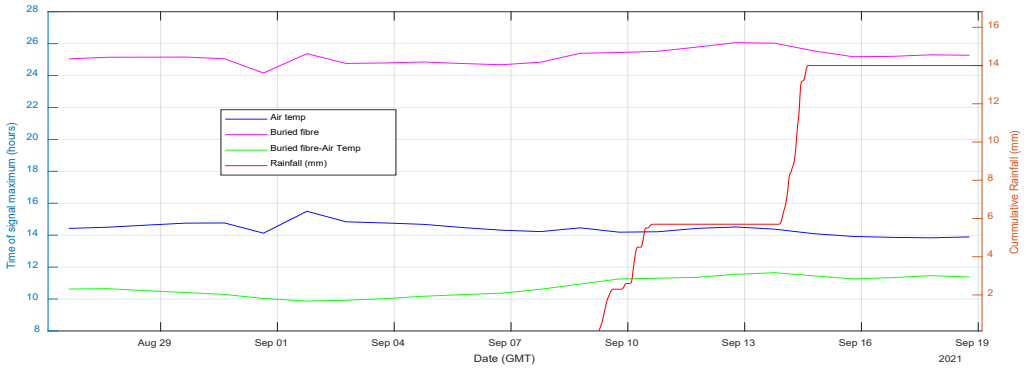

Figure 3: Times of temperature maximum in diurnal cycle.

The diurnal phase difference between the temperature change measured on the fibre at Hollin Hill and the ambient temperature measured on the COSMOS weather station (Stanley et al., 2021) can be used to estimate the diffusivity of the ground for a known burial depth. The burial depth of the fibre at Hollin Hill is around 10 cm but varies across the slope due to the condition of the ground when initially buried and movement of the slope over time. The diffusivity was calculated over a period from 26 March 2021 to 05 April 2021 assuming a constant burial depth and mapped onto the fibre route as shown in the image on the left of Figure 4. If the diffusivity were constant across the slope the calculated burial depth would be as shown in the right-hand image of Figure 4.

The apparent diffusivity also includes the effects of vegetation, so the lack of vegetation across the top of the slope for example results in a higher apparent diffusivity in that region. Higher apparent diffusivity is also seen in isolated areas of the scarp region, particularly in the dual fibre leg where the fibre had moved closer to the surface with time; the burial depth plot on the right of the figure shows that the depth is nearly zero, as the fibre is almost on the surface due to tension between the top and bottom of the scarp pulling the fibre out of the ground. There is also a change in the middle of the slope vertically, which may be a feature of a change in the soil type. The pattern of the measured diffusivity/burial depth across the fibre remains largely constant with time.

Figure 4: Left: calculated thermal diffusivity of the ground above the fibre mapped onto the slope, assuming a constant burial depth. Right: calculated burial depth of the fibre, assuming a constant thermal diffusivity.

Atmospheric pressure changes

Typical fibre does not have a strong response to pressure, but the effects of atmospheric pressure changes have been observed on the fibre. The Hunga Tonga volcano eruption on 15th January 2022 sent pressure waves around the world, which took around 14 hours to reach the slope at Hollin Hill via the North Pole and around 21 hours via the South Pole. The pressure wave arrivals could be seen clearly on barometers in the UK. The atmospheric pressure readings on the weather station at Hollin Hill at the time of recording did not have a high enough time resolution to observe the features of the pressure wave, but pressure readings taken in Fleet, Hampshire in the south of England around 200 miles away show a good correlation to changes across the fibre buried on the slope.

The image to the left of Figure 5 shows the rate of change of phase calculated between samples 24 s apart on the fibre during the event. The response varies depending on the position of the fibre in the ground and the precise nature of the disturbance is not yet explained. The phase of the signal is inverted for some sections, for example. The average phase change measured on the fibre during the disturbance after adjusting for the phase inversions is on the right of Figure 5 along with the measured pressure. The pressure measurement was made around 200 miles from the slope and the time for the pressure wave to travel that distance is around 15 minutes, which is the approximate lag in the signal compared to the fibre output; this is adjusted in the figure to aid the comparison. The correlation with pressure is very clear, but the amplitude of the signal on the fibre is much higher than expected. A typical pressure response of fibre cable with a 4 m gauge length as used here, is less than 1 mrad/Pa, but the average response in this event is around 30 mrad/Pa.

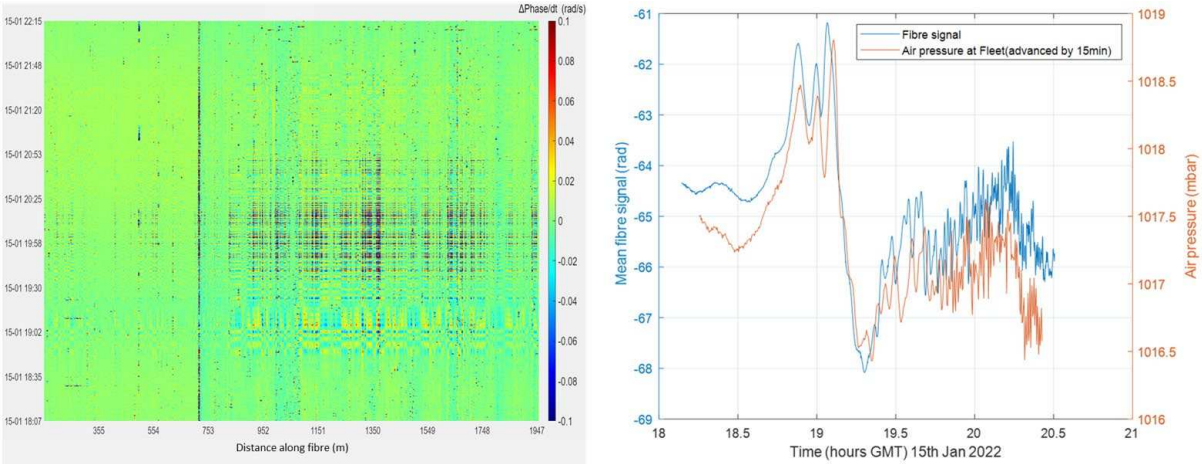

Figure 5: Left – Rate of change of phase observed on the DRS system during the arrival of a pressure wave from the Hunga Tonga volcano. Right – Average phase measured on the fibre on the slope and air pressure during the event.

Surface wave velocities

The effects measured in the sections above are largely caused by changes in the ground above or in the immediate vicinity of the fibre. It is possible to probe deeper into the ground with the DRS system using seismic analysis techniques. Shear wave velocity of surface seismic waves in the near surface can be estimated using surface wave analysis. Surface waves can be generated by an active source such as a sledgehammer or by correlating ambient noise to create virtual source gathers as shown in Figure 6, along with dispersion images showing the surface wave velocity as a function of frequency. Dispersion images can be inverted to give the velocity as a function of depth. Velocities can be estimated at different times to look for time-lapse velocity changes that could correlate with changing moisture content or landslide movement.

Shear wave velocity profiles for one fibre optic line running vertically on the slope are shown in Figure 7 for February 16 and March 2 of 2022, at the start and end of a period of wet weather. There are apparent changes in the velocity field. Change in Gravimetric Moisture Content (GMC) measured on the ERT array is shown in Figure 8 for the same time period along with the time-lapse velocity change. There is good agreement between the GMC change data and the time-lapse velocity change over a depth range of 3 to 10 metres.

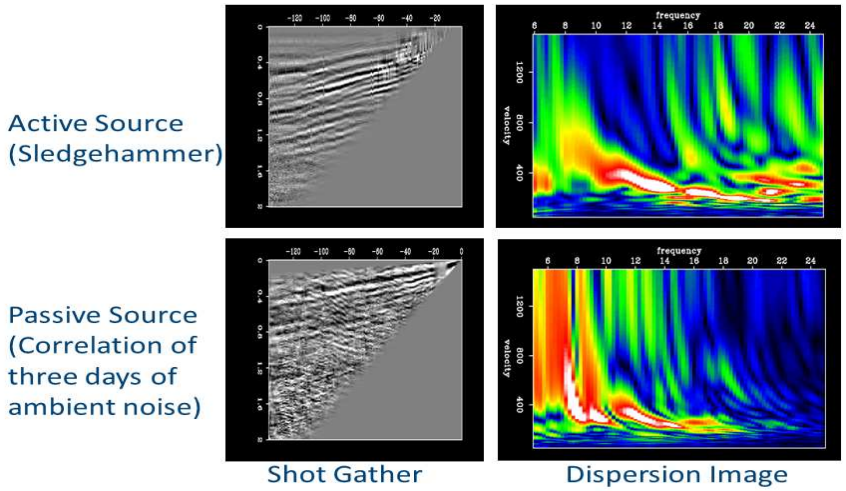

Figure 6: Active and passive shot gathers and associated dispersion images which can be inverted to construct velocity profiles.

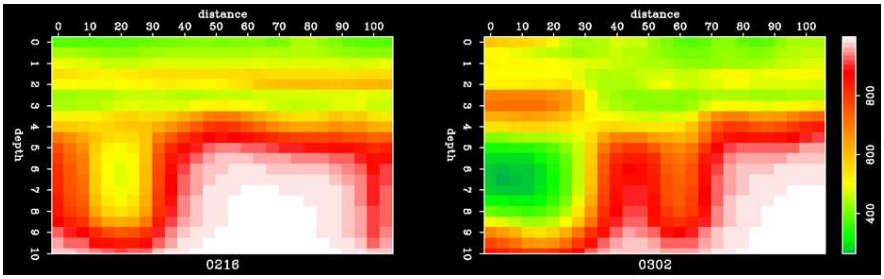

Figure 7: 2D shear wave velocity profiles computed along one fibre line for 16 February and 02 March 2022. Several large storms occurred over this interval, impacting the shallow velocities.

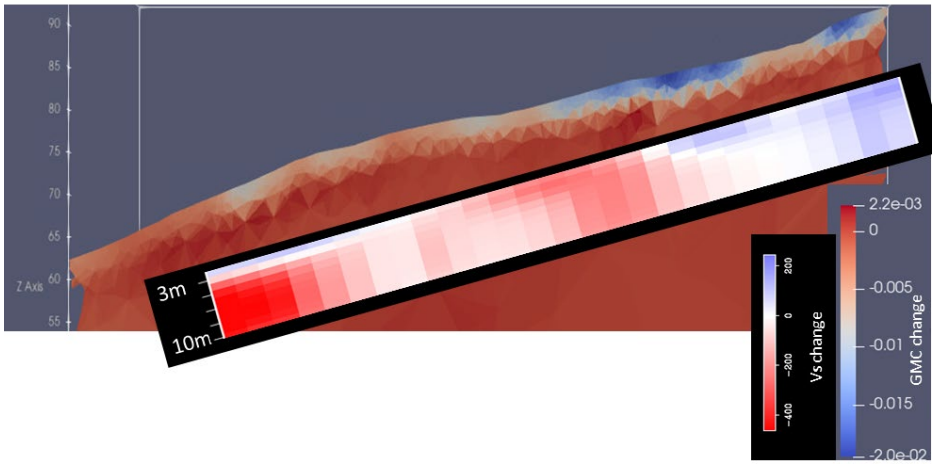

Figure 8: Gravimetric moisture content change over a two-week interval, and in the foreground, shear wave velocity change for the same period. There is good qualitative agreement between shallow velocity change and changing moisture content.

4. Conclusions

It has been shown that fibre optic sensing can be a powerful tool for geotechnical analysis. The high spatial resolution and sensitivity of such systems allows the sub-surface to be studied in greater detail. In addition to traditional measurements of strain, temperature and vibration, a wide range of properties can be inferred, and DRS systems in particular can combine strain and temperature measurements over a wide frequency range (from µHz to kHz) to provide an unprecedented multi-dimensional picture of sub-surface properties and slope behaviour. The immediate availability of the data and rapid response of the system provides the opportunity for effective early warning systems of events such as landslides, in addition to longer term analysis.

Brief examples of some of the analysis possibilities was presented, further work is required to fully understand some of the behaviour seen on the fibre to events such as pressure changes and to correctly interpret thermal and seismic data with regards to properties of the sub-surface.

References

Andújar Márquez, J.M., Martínez Bohórquez, M.Á., Gómez Melgar, S. (2016). Ground thermal diffusivity calculation by direct soil temperature measurement. Application to very low enthalpy geothermal energy systems. *Sensors*, vol. 16:306. https://doi.org/10.3390/s16030306

Clarkson, P., Crickmore, R., Godfrey, A., Minto, C., Chambers, J., Dashwood, B., Gunn, D., Jones, L., Meldrum, P., Morgan, D., Watlet, A. and Whiteley, J. (2021a). Correlation between Distributed Rayleigh Sensing (DRS) and moisture sensors as indicators of slope instability. In *Proc. EAGE Near Surface Geoscience,* Bordeaux, European Association of Geoscientists and Engineers.

Clarkson, P., Minto, C., Crickmore, R., Godfrey, A., Purnell, B., Chambers, J., Dashwood, B., Gunn, D., Jones, L., Meldrum, P., Watlet, A. and Whiteley, J. (2021b). Distributed Rayleigh Sensing for slope stability monitoring. In *Proc. 55th US Rock Mechanics/ Geomechanics Symposium*, Houston, TX. American Rock Mechanics Association.

Crickmore, R., Minto, C. and Godfrey, A. (2020). Temperature and strain separation from a Distributed Rayleigh Sensing system. In *Proc. EAGE Workshop on Fibre Optic Sensing for Energy Applications*, Malaysia, European Association of Geoscientists and Engineers.

Stanley, S., Antoniou, V., Askquith-Ellis, A., Ball, L.A., Bennett, E.S., Blake, J.R., Boorman, D.B., Brooks, M., Clarke, M., Cooper, H.M., Cowan, N., Cumming, A., Evans, J.G., Farrand, P., Fry, M., Hitt, O.E., Lord, W.D., Morrison, R., Nash, G.V., Rylett, D., Scarlett, P.M., Swain, O.D., Szczykulska, M., Thornton, J.L., Trill, E.J., Warwick, A.C., Winterbourn, B. (2021). Daily and sub-daily hydrometeorological and soil data (2013-2019) [COSMOS-UK]. NERC Environmental Information Data Centre.

Uhlemann, S., Chambers, J., Wilkinson, P., Maurer, H., Merritt, A., Meldrum, P., Kuras, O., Gunn, D., Smith, A., Dijkstra, T. (2017). Four-dimensional imaging of moisture dynamics during landslide reactivation. *Journal of Geophysical Research: Earth Surface*, 122: 398-418.